tory bulb (five rats) (Fig. 2A).

Finally, attempting to dissociate the f-EPSP changes from the exploratory behavior, we used radiant heat to bring the brain temperature to the maximum value that was obtained during exploration on the previous day. By intermittent infrared heating, the brain temperature was kept just above this temperature (Fig. 3A, middle). In five of five rats, exploratory activity had normal intensity under these conditions, but no further change in the f-EPSP was observed (Fig. 3A). Input-output tests (as in Fig. 1B) showed that the lack of additional changes in the f-EPSP was not due to a ceiling effect. In another series of experiments, the brain was warmed before the exploration. The magnitude of the exploration-induced potential changes depended on the increment in brain temperature and disappeared altogether at a sufficiently high starting temperature (Fig. 3B). Again, the exploratory intensity was unchanged from that of the control sessions. The dissociation of the exploratory behavior from the f-EPSP changes argues against a causal relation between the two processes.

Our results show a consistent relation between the field potential parameters and brain temperature, whether the latter is changed by heat produced by muscle activity or by artificial warming. In essence, the observed f-EPSP changes during exploration appear to be caused primarily by an increased brain temperature due to muscular heat production rather than by a learning-induced change in synaptic strength. The results represent a caveat for the interpretation that in freely moving rats changed f-EPSPs are signs of altered synaptic efficiency. They do not rule out the possibility that f-EPSP changes are produced by learning but they do indicate that such changes must be evoked independently of changes in brain temperature that are induced by activity, environment, or drugs.

REFERENCES AND NOTES

1. C. A. Barnes, *Trends Neurosci.* **11**, 163 (1988); J. O'Keefe and L. Nadel, *The Hippocampus as a Cognitive Map* (Clarendon, Oxford, 1978).
2. R. Morris and M. Baker, in *Neuropsychology of Memory*, L. Squire and N. Butters, Eds. (Guilford, New York, 1984), pp. 521–535; E. L. Hargreaves, D. P. Cain, C. H. Vanderwolf, *J. Neurosci.* **10**, 1472 (1990).
3. P. E. Sharp, B. L. McNaughton, C. A. Barnes, *Psychobiology* **17**, 257 (1989); E. J. Green, B. L. McNaughton, C. A. Barnes, *J. Neurosci.* **10**, 1455 (1990).
4. P. Andersen, *Acta Physiol. Scand.* **48**, 209 (1960); S. M. Thompson, L. M. Masukawa, D. A. Prince, *J. Neurosci.* **5**, 817 (1985); S. J. Schiff and G. G. Somjen, *Brain Res.* **345**, 279 (1985); K. Shen and P. A. Schwartzkroin, *ibid.* **475**, 305 (1988).
5. During exploration there was an unexpected relation between the f-EPSP and the population spike. Normally, when the f-EPSP increases the population spike grows and its latency diminishes. The paradoxical spike amplitude reduction with reduced latency during exploration is probably an effect of increased brain temperature. The larger f-EPSP and its shorter latency are both probably caused by a temperature-induced increased speed of transmitter release [B. Katz and R. Miledi, *J. Physiol. (London)* **181**, 656 (1965)], an effect of physiological significance. The reduced spike latency results from the f-EPSP increase. The effects of warming and of cooling on the population-spike amplitude are exactly opposite. Cooling gives three effects: (i) a small depolarization lowers the threshold for cell discharges, which causes more cells to fire; (ii) each discharging cell contributes a larger signal [A. L. Hodgkin and B. Katz, *J. Physiol. (London)* **109**, 240 (1949)]. and (iii) because each action potential in the cooled state is broader than it is in the warm condition [G. M. Schoepfle and J. Erlanger, *Am. J. Physiol.* **134**, 694 (1941)], the algebraic summation of the individual units to a compound potential results in a larger sum, in spite of the fact that the onset times are more spread out (less synchronous) than they are in the warm condition.
6. R. Abrams and H. T. Hammel, *Am. J. Physiol.* **206**, 641 (1964); *ibid.* **208**, 698 (1965); C. J. Gordon, *Physiol. Behav.* **47**, 963 (1990).
7. R. M. Abrams, J. A. J. Stolwijk, H. T. Hammel, H. Graichen, *Life Sci.* **4**, 2399 (1965); M. A. Baker, *Annu. Rev. Physiol.* **44**, 85 (1982).
8. Male Long Evans rats (250 to 500 g) were anesthetized with a mixture of chloral hydrate and pentobarbital (Equithesin, 1.0 ml per 250 g of body weight). Bipolar stimulation electrodes (SNEX 100; Rhodes Medical, Woodland Hills, CA) were implanted in the right angular bundle (7.5 to 8.0 mm posterior and 4.3 mm lateral to bregma), and a tungsten recording electrode was placed in the dentate hilus or granule cell layer (4.0 mm posterior and 2.6 mm lateral to bregma). Responses in the CA1 pyramidal layer to stimulation of Schaffer collaterals or olfactory bulb responses to lateral olfactory tract stimulation were recorded in some animals. A thermistor (0.5-mm diameter; 111-802 EAJ-B01, Fenwal Electronics, Milford, MA) was implanted contralaterally at the homotopic point of the recording electrode. Electrode and thermistor leads were connected to a socket fastened to the skull with dental acrylic. Before implantation, each thermistor was calibrated in a water bath against a precision thermometer. The thermistors allowed temperatures to be measured at a precision of 0.05° to 0.1°C. The rats were allowed 1 week of recovery before testing started. Behavioral testing was performed at 23°C (air temperature) and began 1 to 2 hours after the rat was connected to the recording equipment, when both the electrical and temperature records had reached stable values. Test f-EPSPs were elicited by a constant stimulus (100 to 500 μA, 50 μs) at 0.2 or 0.07 Hz. The slope of the f-EPSP was measured near its maximum as the amplitude difference at two fixed latencies. The population spike was taken as the vertical distance between the peak and a joint tangent to the preceding and succeeding positivities. The spike latency was defined as the time from stimulus onset to the spike peak.
9. R. G. M. Morris, *J. Neurosci. Methods* **11**, 47 (1984).

10. We thank T. Eriksen, E. Aaboen Hansen, B. Piercey, and T. Reppen for technical assistance. Supported by the Norwegian Medical Research Council.

11 September 1992; accepted 25 November 1992

Higher Level Organization of Individual Gene Transcription and RNA Splicing

Yigong Xing, Carol V. Johnson, Paul R. Dobner, Jeanne Bentley Lawrence*

Visualization of fibronectin and neurotensin messenger RNAs within mammalian interphase nuclei was achieved by fluorescence hybridization with genomic, complementary DNA, and intron-specific probes. Unspliced transcripts accumulated in one or two sites per nucleus. Fibronectin RNA frequently accumulated in elongated tracks that overlapped and extended well beyond the site of transcription. Splicing appears to occur directly within this RNA track, as evidenced by an unambiguous spatial separation of intron-containing and spliced transcripts. Excised introns for neurotensin RNA appear free to diffuse. The transcription and processing site of the fibronectin gene localized to the nuclear interior and was associated with larger transcript domains in over 88 percent of the cells. These results support a view of nuclear function closely integrated with structure.

The long-standing interest in the spatial organization of transcription and splicing within the interphase nucleus has been heightened by several observations (*1*). Visualization by fluorescence microscopy of highly localized nuclear "tracks" of specific viral RNAs (*2*), preserved in chromatin-depleted nuclear matrix extracts (*3*), indicated that these RNAs are not free to diffuse but rather are associated with an underlying nuclear substructure (*4*). The results of an autoradiographic study have indicated that intron sequences in acetylcholine receptor mRNA preferentially localize around the nuclear periphery (*5*). Total nuclear polyadenylate [poly(A)] RNA has been shown to accumulate within 20 to 40 discrete "transcript domains" that coincide with the location of small nuclear ribonucleoproteins (snRNPs) (*6*, *7*). These snRNPs were previously reported to exhibit a clustered nuclear distribution (*8*) coincident with the spliceosome assembly factor SC-35 (*9*). The concentration of microinjected globin RNA within these 20 to 40

Y. Xing, C. V. Johnson, J. B. Lawrence, Department of Cell Biology, University of Massachusetts Medical Center, 55 Lake Avenue North, Worcester, MA 01655. P. R. Dobner, Department of Molecular Genetics and Microbiology, University of Massachusetts Medical Center, 55 Lake Avenue North, Worcester, MA 01655.

*To whom correspondence should be addressed.

regions (*10*) contrasts with its marked localization to one or two nuclear sites, as observed for several viral RNAs (*2, 11*) and for c-*fos* RNA synthesized in vivo (*12*). Defined localization of an RNA suggests an association with nuclear substructure. Using a combination of intron, cDNA, and genomic probes for simultaneous RNA-DNA hybridization, we have visualized the intranuclear distribution of endogenous RNAs, related this distribution to sites of transcription and processing, and related these sites to larger domains enriched in poly(A) RNA and splicing factors.

We first studied the transcripts from the inducible gene for a neuropeptide, neurotensin, in PC-12 cells (*13*) by means of a genomic probe spanning the 10-kb gene (Fig. 1A). Approximately 4 hours after induction, positive cells showed either one (42%) or two (58%) distinct foci of intense nuclear fluorescence (Fig. 2A) and a diffuse, less intense signal often apparent throughout the cytoplasm and nucleoplasm. Elongated tracks for neurotensin nuclear RNA were not observed from any orientation (Fig. 2). Neither the nuclear nor cytoplasmic signals were detectable in uninduced PC-12 cells. We also studied the localization of RNA for the extracellular matrix glycoprotein fibronectin (*14*) in rat RFL-6 fibroblasts and L6 myoblasts with a 6.5-kb genomic probe (Fig. 1B). Up to 80% of the nuclei showed one or two distinct sites of intense hybridization, which is indicative of accumulated fibronectin nuclear RNA. This was confirmed by controls showing that the hybridization was to RNA (*15*). Interestingly, the fibronectin RNA frequently accumulated in tracks (Fig. 2D) up to 6 μm long that in some cells extended through several planes of focus. Both the length and orientation of the tracks with respect to the *x*-*y* and *z* axes were highly variable (*16*).

To investigate whether the concentrated RNA signals detected with genomic probes represented unprocessed transcripts, mature mRNA, or excised introns, we performed in situ hybridization with intron-specific and cDNA probes. When the same labeling method was used on separate cell samples, both cDNA and intron probes hybridized to just one or two focal sites within the nuclear interior (Fig. 2, B and C). Two-color labeling experiments showed that for both fibronectin (Fig. 2, E and F) and neurotensin RNAs the cDNA and intron probes hybridized to the same nuclear foci, which indicates the presence of unspliced transcripts.

Localized concentrations of specific nuclear RNAs could represent the site of any rate-limiting step along the progression from transcription to processing to translocation through nuclear pores. To determine whether fibronectin RNA accumulations colocalized with the sites of transcription, we examined the spatial relationship of the gene and the RNA, focusing on fibronectin RNA because of its more elongated RNA track. This was accomplished by two-color hybridization in situ with a 4.3-kb probe for the nontranscribed 5′ sequence immediately flanking the fibronectin gene and a 6.5-kb probe (Fig. 1B) for genomic DNA. Using methods for precise registration of different color fluorochromes (Fig. 3), we found that the gene and the RNA focus or track were spatially coincident (Fig. 3, A and B). For 86% of the gene signals detected (n = 88), there was an overlap between the gene and an RNA track. Furthermore, in 88% of the RNA tracks the gene was clearly positioned at or near one end. This polarity was apparent even within focal (nonelongated) accumulations of fibronectin RNA (Fig. 3B). These results suggest that RNA tracks form directly at the site of transcription and indicate a structural polarity to the RNA formation with the gene toward one end. Because the length of the gene is below the resolution of the light microscope and therefore produces just a point signal of fluorescence (*17*), the longer RNA formations observed do not represent a "Christmas tree" of nascent transcripts synthesized along the DNA template (as has been identified for *Drosophila melanogaster* ribosomal DNA and amplified chorion genes by electron microscopy) (*18*) but rather an accumulation of many RNA molecules that extend well beyond the dimensions of the gene.

The site of RNA processing and the spatial relation between RNA processing and transcription in mammalian nuclei are not yet established (*19*). Hence, it was important to discriminate between fundamentally different hypotheses to explain the RNA accumulation at the site of transcription; for example, the accumulation could represent a buildup of newly synthesized transcripts before transport elsewhere for processing or it could represent an "assembly line" of transcripts that undergo processing at or near the transcription site. Evidence for the latter hypothesis came from two-color hybridization experiments with cDNA and intron probes by techniques that allowed precise registration of the two colors. Hybridization with the fi-

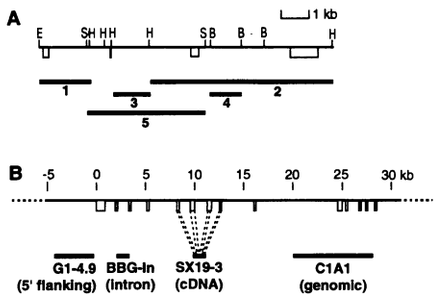

Fig. 1. Hybridization probes for neurotensin and fibronectin RNAs. (**A**) Map of the rat neurotensin gene (~10 kb). The black bars indicate the hybridization probes, and the open boxes indicate exons. Transcription starts 100 nucleotides upstream of the first exon. Eco RI (E), Bam HI (B), Hind III (H), and Sac I (S) restriction sites are shown. The genomic probe used in the initial hybridizations was a pool of probes 1, 2, and 5. For detection of exons only, a full-length cDNA clone for the 1-kb mRNA (*13*) was used. (**B**) Map of the rat fibronectin gene (~30 kb). The scale is marked in kilobases from the transcription initiation site. The black bars indicate the fibronectin probes and the open boxes indicate exons. We subcloned the G1-4.9 and BBG-In probes to obtain 5′ flanking and intron sequences devoid of exons.

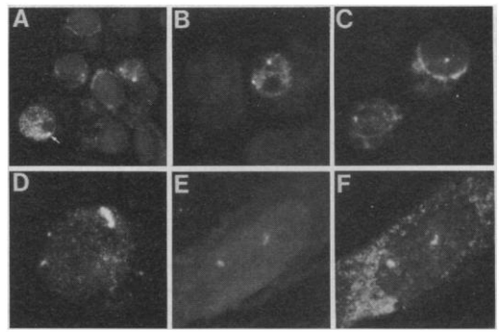

Fig. 2. Detection of neurotensin and fibronectin RNAs as described (*15*). Neurotensin RNA was detected in rat PC-12 cells 4 hours after induction (*15*), and fibronectin RNA was detected in rat RFL-6 fibroblasts. (**A**) Neurotensin genomic probe (Fig. 1A). One or two bright foci (arrow) were observed in the nucleus of positive cells, with less intense diffuse nucleoplasmic signal. (**B**) Neurotensin intron-specific probe 3 (Fig. 1A) showing two foci, with dimmer, slightly punctate fluorescence throughout the nucleoplasm excluding the nucleolus. (**C**) Neurotensin RNA exon-specific (cDNA) probe, showing one or two bright nuclear foci with less intense signal also in the cytoplasm. (**D**) Fibronectin genomic probe C1A1 (Fig. 1B), showing highly elongated nuclear RNA track of rat fibroblast. In this experiment there were one, two, or more than two intense sites of hybridization in 55%, 40%, and 5% of nuclei, respectively. (**E**) Fibronectin RNA hybridized with digoxigenin-labeled, intron-specific probe BBG-In (Fig. 1B) and detected with rhodamine. (**F**) Fibronectin RNA hybridized with biotin-labeled, exon-specific cDNA probe SX19-3 (Fig. 1B) and detected with fluorescein isothiocyanate (FITC)–avidin in the same cells shown in (E). Final magnifications: (A), (B), and (C), ×2000; (D), (E), and (F), ×1800.

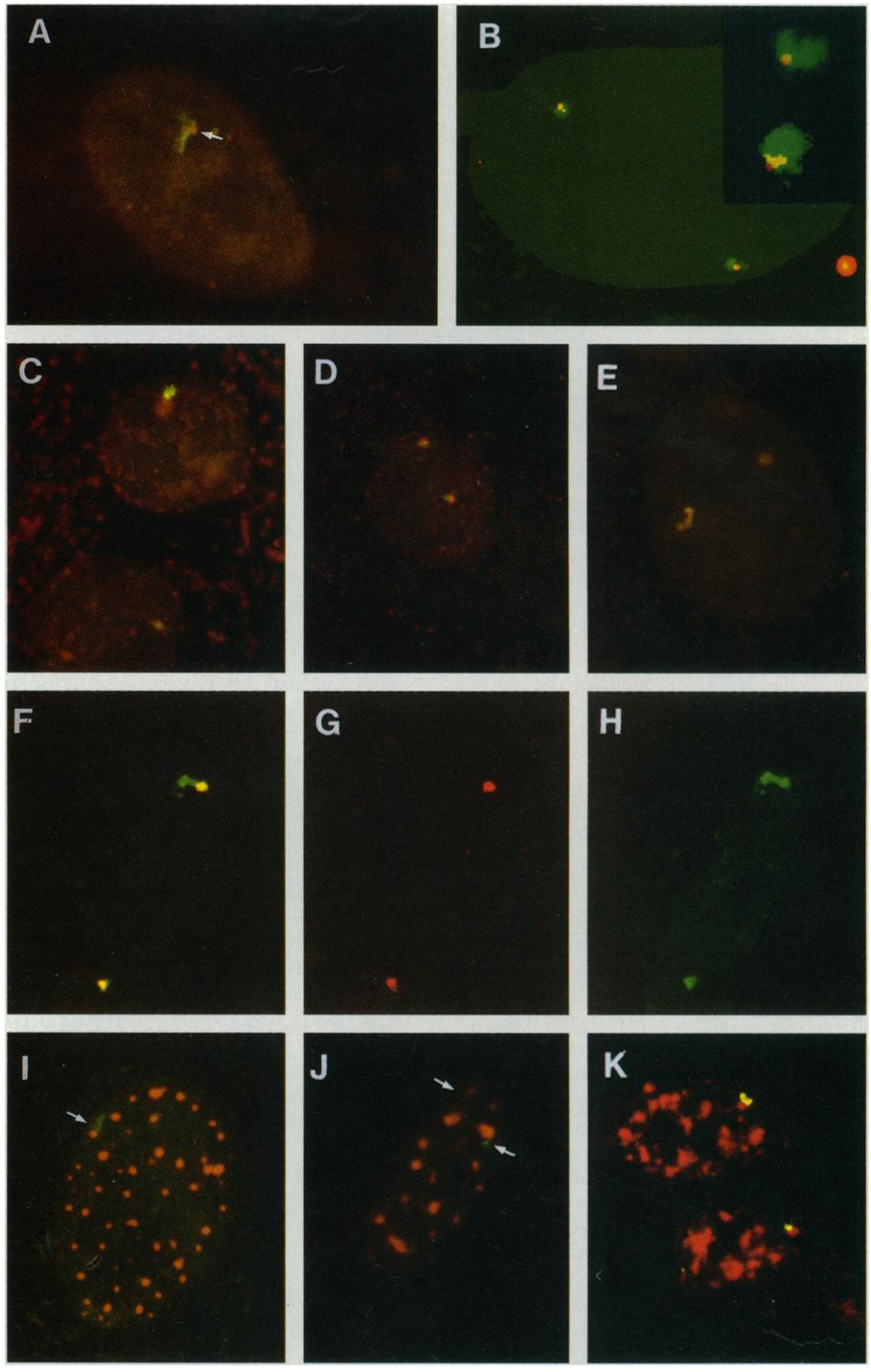

Fig. 3. Location of fibronectin RNA tracks relative to sites of transcription, splicing, and larger transcript domains. (**A** and **B**) Nuclear location of the fibronectin gene and its primary transcripts shown by dual-label hybridization on RFL-6 fibroblasts. Probe G1-4.9, which contains 4.3 kb of nontranscribed 5′ flanking sequence of the rat fibronectin gene, was labeled with digoxigenin (red, rhodamine). The RNAs were visualized by hybridization with a biotinylated C1A1 genomic probe (green, FITC). Fixed cells were denatured and hybridized as described (*15*). The photomicrograph in (A) was taken through a dual-band filter that allows precise alignment of red and green fluorescence (arrow denotes the gene signal). The image in (B) was captured by a CCD camera from separate filters superimposed and aligned with multicolor fluorescence beads (lower right) as fiduciary markers. The inset shows two additional examples. (**C**) Fibronectin gene transcripts detected by the biotinylated intron probe BBG-In (green, FITC) and by the digoxigenin cDNA probe SX19-3 (red, rhodamine). The cDNA signal extended further than the intron signal. (**D**) Reverse labeling to (C) (BBG-In, digoxigenin, rhodamine; SX19-3, biotin, fluorescein). (**E**) Hybridization of probes for the same sequence (C1A1) labeled with biotin and digoxigenin show no color separation. Separate CCD images of (**F**) both exon and intron, (**G**) intron, and (**H**) exon show exon sequences that extend through the whole track. (**I** and **J**) Location of the fibronectin RNA tracks (arrows) or foci relative to transcript domains visualized with antibodies to SC-35 (*9*) in WI-38 fibroblasts. Digoxigenin-labeled 2-kb pFH-1 human cDNA probe is shown in green and antibody to SC-35 is shown in red. In our experiments, SC-35 did not react with rat cells. (**K**) Fibronectin RNA tracks (green) relative to transcript domains visualized by poly(A) RNA hybridization with a biotinylated deoxy$(T)_{55}$ probe (red) (*6*). Final magnifications: (A), ×1800; (B), ×2500; (C) through (K), ×1800.

bronectin cDNA probe produced signals that formed longer tracks than those formed with the intron probes in 84% of cells (Fig. 3, F to H). Within a single cell, the intron signal was generally confined to a smaller part of the track than the exon signals, which thereby created the appearance of a two-color track. This segmented track was consistently observed with two different analytical methods, one that used a single filter set that allowed simultaneous visualization of red and green with no optical shift (*20*, *21*) (Fig. 3, C and D) and a second that used separate images captured by a cooled CCD (charge-coupled device) camera that were aligned and superimposed (Fig. 3, F to H). In several control experiments in which a single probe was labeled in two colors, there was no separation of the red and green signals (Fig. 3E). The absence of intron sequences from a portion of the focus or track defined by the cDNA probe indicates that intron splicing occurs within this accumulation of RNA. Further, these results suggest that the splicing process is spatially ordered within the track (Fig. 4).

As initially observed with genomic probes (Fig. 2, A and D), hybridization with intron probes also produced a less intense, slightly punctate fluorescence dispersed throughout the nucleoplasm, excluding the nucleolus. This was most clear for neurotensin RNA (Fig. 2, A to C), where two probes for different introns produced both bright foci and widespread dim fluorescence in the nucleus with essentially no label in the cytoplasm. This dispersed signal was not detected with cDNA probes of similar size. The nucleoplasmic intron signal was detectable only in induced cells that expressed bright fluorescent foci of neurotensin RNA (Fig. 2). Similarly, hybridization with genomic or intron probes for fibronectin RNA frequently showed more nucleoplasmic staining (Fig. 2D), although this was not found as consistently as it was for neurotensin RNA, possibly for technical reasons (*22*). For both RNAs, the dimmer intron signal was distributed rela-

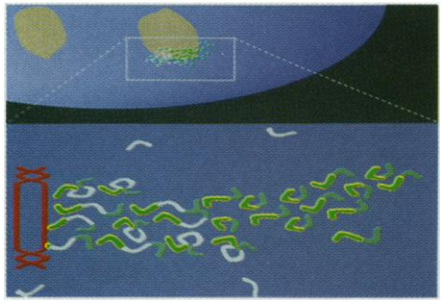

Fig. 4. Schematic model for the ordered assembly of transcripts within the fibronectin RNA track. This model suggests that transcripts at different stages of processing are concentrated in different areas along a processing track at varying distances from the gene. During splicing, the unprocessed transcripts do not appear to be freely diffusing but rather may be physically associated with an insoluble nuclear substructure. A simplified version of the primary transcript is shown, with a single intron indicated in white and exons indicated in green. The exon probe used in these experiments is highlighted with yellow to indicate its position 3′ to the intron probe (white). The schematic shows the RNA track oriented with the intron-containing transcripts closest to the gene, although this has not been directly demonstrated.

	Poly(A)	SC-35
Completely coincident	8%	3%
Partially overlapping	43%	23%
In contact	37%	42%
Separate	12%	32%

Fig. 5. Quantitative summary of the spatial relation between fibronectin RNA foci or tracks and transcript domains. Open circular structures represent signals from deoxy$(T)_{55}$ hybridization or antibody staining of SC-35 domains. Patched areas represent signals from pFH-1 hybridization to human WI-38 fibroblasts. Nuclei (n = 130) were scored by two independent investigators. The first three categories represent different positional relations of tracks or foci that were associated (in contact) with bigger transcript domains, totaling 88% for poly(A) RNA and 68% for SC-35. If tracks and domains did not appear to be in contact, they were scored as separate (regardless of the distance between them). This analysis was performed with optics (Zeiss Neofluor 100, 1.4 numerical aperture) that allow 0.5-μm z axis resolution. In addition, several cells were serially sectioned in 0.2-μm optical steps.

tively uniformly and did not concentrate around the nuclear periphery, as reported previously for some introns localized by autoradiography (*5*). The apparent free diffusion of intron sequences agrees with biochemical fractionation and Northern (RNA) blot analyses (*23*), which indicated that excised introns are more abundant than previously inferred in studies of detergent-extracted cells. This is because the introns are more easily extracted from the nucleus, whereas the primary transcripts and the processed mRNA remain insoluble within the matrix fraction.

We next investigated the distribution of fibronectin RNA relative to transcript domains (*6*). Two different overlapping probes were used to define such transcript domains (*6, 7*): oligo(dT) to detect poly(A) RNA and an antibody to the spliceosome assembly factor SC-35 (*9*). Quantitative analysis of >100 cells by direct microscopic visualization through a dual-band filter (Fig. 3, I and J) or by superimposed computer images of optically sectioned cells captured from a CCD camera (Fig. 3K) showed a variable but nonrandom spatial relation between fibronectin RNA foci or tracks and the larger domains enriched in SC-35 and poly(A) RNA. Approximately 88% of fibronectin RNA tracks or foci were associated with poly(A) RNA-rich domains, with the vast majority either partially overlapping or immediately juxtaposing the domain (Fig. 5). Only a small fraction of the tracks were completely within the domain. The association of fibronectin RNA with transcript domains is highly specific (*24*). Although the pattern of colocalization was similar to that of SC-35 (Fig. 3, I to K), the fraction of fibronectin RNA tracks separate from a visible transcript domain increased from 12 to 32% (Fig. 5). Consistent with the observation that SC-35 forms a smaller inner core (*6*), some tracks may overlap the periphery of poly(A) domains without contacting the SC-35 core. In five optically sectioned cells, the fibronectin RNA accumulations did not extend to the nuclear envelope but were positioned in the same focal planes as transcript domains, within the nuclear interior. It remains to be determined how the RNA track is oriented relative to the transcript domain and the nuclear envelope and whether fibronectin gene transcription occurs just within or immediately next to the transcript domain.

By directly localizing the site of individual gene transcription and splicing and their relation to larger poly(A)- and snRNP-rich domains, we provide evidence for a view of RNA metabolism as it relates to nuclear structure within mammalian cells. Allelic genes from homologous chromosomes are commonly both transcriptionally active and spatially separate. Unprocessed RNA molecules do not freely diffuse but rather accumulate at the site of transcription. The excision of introns occurs within this accumulation of RNA, and this may be in "assembly line" fashion along a polarized track that begins at the site of transcription (Fig. 4). The order evident within the track strongly suggests that the RNA is physically associated with a nuclear substructure. In contrast, excised introns for at least some RNAs appear free to diffuse. Tracks of fibronectin RNA, representing sites of both transcription and splicing, partially overlap or immediately juxtapose larger transcript domains, which show a specific spatial configuration within the nucleus (*6*). Although some RNA transport is likely to occur along this track, perhaps at the same time as processing, our observation that fibronectin RNA tracks or foci did not generally extend to the nuclear envelope leaves open the possibility that transport of mature mRNA, which may be quite rapid, occurs along more than one route or even by free diffusion.

Given the number, relative size, and intensity of the signals for poly(A) RNA domains versus the signals for specific RNAs (*25*), it is likely that each transcript domain reflects the transcription and processing activity of several different genes. If other active genes are found to be preferentially positioned relative to these domains, this may have profound implications for the regulation of gene expression and the organization of the genome. The observed accumulation of c-*fos* transcripts near snRNP-rich domains (*12*) is consistent with this suggestion as are recent results of experiments aimed at localizing primary transcripts from several other genes (*26*). Whether nuclear transcripts from a given gene form a focus, track, or highly elongated track [as seen with certain viral RNAs (*3, 4*)] may depend largely on the amount of processing the primary transcript must undergo and the efficiency with which both processing and transport occur. In contrast to microinjected precursor mRNAs, which apparently can freely diffuse throughout the nucleus (*10*), our data show that genes and their precursor mRNAs synthesized in vivo exhibit both higher level nuclear organization as well as a functional association with the underlying substructure.

REFERENCES AND NOTES

1. S. Fakan and E. Puvion, *Int. Rev. Cytol.* **65**, 255 (1980); J. G. Gall, *Science* **252**, 1499 (1991); D. A. Jackson, *BioEssays* **13**, 1 (1991); G. Blobel, *Proc. Natl. Acad. Sci. U.S.A.* **82**, 8527 (1985); R. Van Driel, B. Humbel, L. de Jong, *J. Cell. Biochem.* **43**, 311 (1991); D. Comings, *Hum. Genet.* **80**, 131 (1980).
2. J. B. Lawrence, R. H. Singer, L. M. Marselle, *Cell* **57**, 493 (1989).
3. Y. Xing and J. B. Lawrence, *J. Cell Biol.* **112**, 1055 (1991).
4. R. Berezney and D. S. Coffey, *Biochem. Biophys. Res. Commun.* **60**, 1410 (1974); E. M. Ciejek, M.-J. Tsai, B. W. O'Malley, *Nature* **306**, 607 (1983); E. G. Fey, D. A. Ornelles, S. Penman, *J. Cell Sci. Suppl.* **5**, 99 (1986); H. Gallinaro, E. Puvion, L. Kister, M.

Jacob, *EMBO J.* **2**, 953 (1983); D. Jackson and P. Cook, *ibid.* **7**, 3667 (1988).
5. S. A. Berman, S. Bursztajn, B. Bowen, W. Gilbert, *Science* **247**, 212 (1990).
6. K. C. Carter *et al.*, *ibid.* **259**, 1330 (1993).
7. K. C. Carter, K. L. Taneja, J. B. Lawrence, *J. Cell Biol.* **115**, 1191 (1991).
8. D. L. Spector, W. H. Schrier, H. Busch, *Biol. Cell* **49**, 1 (1983); S. Fakan, G. Leser, T. E. Martin, *J. Cell Biol.* **98**, 358 (1984); N. Ringertz *et al.*, *J. Cell Sci. Suppl.* **4**, 11 (1986); J. D. Northway and E. M. Tan, *Clin. Immunol. Immunopathol.* **1**, 140 (1972).
9. X.-D. Fu and T. Maniatis, *Nature* **343**, 437 (1990).
10. J. Wang, L. Cao, Y. Wang, T. Pederson, *Proc. Natl. Acad. Sci. U.S.A.* **88**, 7391 (1991).
11. J. B. Lawrence, L. M. Marselle, K. S. Byron, J. L. Sullivan, R. H. Singer, *ibid.* **87**, 5420 (1990); A. Raap *et al.*, *Exp. Cell Res.* **197**, 319 (1991).
12. S. Huang and D. L. Spector, *Genes Dev.* **5**, 2228 (1991).
13. P. R. Dobner, A. S. Tischler, Y. C. Lee, S. R. Bloom, S. R. Donahue, *J. Biol. Chem.* **263**, 13983 (1988); E. Kislauskis, B. Bullock, S. McNeil, P. R. Dobner, *ibid.*, p. 4963; M. J. Alexander *et al.*, *Proc. Natl. Acad. Sci. U.S.A.* **86**, 5202 (1989).
14. J. E. Schwarzbauer, R. S. Patel, D. Fonda, R. O. Hynes, *EMBO J.* **6**, 2573 (1987); R. S. Patel, E. Odermatt, J. E. Schwarzbauer, R. O. Hynes, *ibid.*, p. 2565.
15. The methods used here extend a series of studies aimed at improving the preservation and detection of nuclear RNA and DNA in situ [J. B. Lawrence, C. A. Villnave, R. H. Singer, *Cell* **52**, 51 (1988); (*2, 3, 7, 20*)]. For studies on fibronectin RNA, cells were grown and analyzed as monolayers on glass cover slips. Before hybridization, cells were treated for 30 s with 0.5% Triton X-100 in cytoskeleton buffer [E. G. Fey, G. Krochmalinc, S. Penman, *J. Biol. Chem.* **102**, 1654 (1986)] at 4°C to permeabilize nuclei and were then fixed in 4% paraformaldehyde and 1× phosphate-buffered saline for 5 min at room temperature. Cells were stored in 70% ethanol at 4°C before hybridization. Rat PC-12 cells were induced to express neurotensin (*13*) by the addition of nerve growth factor (100 ng/ml), 1 μM Dexamethasone (Sigma), 1 μM forskolin (Sigma), and 10 mM LiCl. Because PC-12 cells have little cytoplasm and are nonadherent on glass, they did not require detergent treatment but were spun from suspension onto cover slips for 5 min at 500 rpm and fixed in 4% paraformaldehyde for 5 to 10 min. Hybridization with the fibronectin and neurotensin probes was performed essentially as described (*2, 20*) with the probe (5 μg/ml) in 50% formamide 2× saline sodium citrate (SSC) for 4 to 16 hours at 37°C. For simultaneous detection of fibronectin RNA and poly(A) RNA, the cDNA probe for fibronectin (pFH-1) was hybridized first and then the oligo(dT) [deoxy$(T)_{55}$; 0.5 μg/ml] was hybridized in 15% formamide and 2× SSC at 37°C for 2 to 3 hours. The monoclonal antibody to SC-35 was used at 37°C for 60 min and then detected with a rhodamine-conjugated donkey antibody to murine immunoglobulin (Jackson ImmunoResearch Labs). Several points support the conclusion that the methods specifically detect nuclear RNA. In the absence of denaturation before hybridization, double-stranded cellular DNA is unavailable for hybridization (*2, 20*). Consistent with this observation in the inducible system (neurotensin), the noninduced cells showed no nuclear signal, and in the fibronectin system, the nuclear RNA signals were removed by alkaline hydrolysis of RNA with NaOH. The larger RNA signals relative to single-copy gene signals and the coincidence in expression of nuclear and cytoplasmic RNA signals provide further evidence that we are detecting nuclear RNA.
16. We have investigated nuclear localization of several other RNAs, including six different viral and cellular precursor mRNAs in different cultured cell types, and have not found evidence for a specific orientation of the RNA tracks. In randomly rotated suspension cells, RNA foci artifactually appeared oriented in the *z* axis because of the limited *z* axis resolution of the confocal microscope. Separation of specific sequences along viral RNA tracks has also been observed (J. B. Lawrence and J. Bauman, unpublished data).
17. As has been documented in detail [J. B. Lawrence, R. H. Singer, J. A. McNeil, *Science* **249**, 928 (1990); B. Trask, D. Pinkel, G. van den Engh, *Genomics* **5**, 710 (1989)], the length of individual genes within interphase nuclei is generally below the resolution of the light microscope (0.1 to 0.2 μm). Even sequences separated by 70 kb (the full length of the fibronectin gene) are less than 0.2 μm apart in approximately 90% of nuclei and therefore appear as a single, small spot.
18. O. L. Miller, Jr., and B. R. Beatty, *Science* **164**, 955 (1969); Y. O. Osheim, O. L. Miller, A. L. Beyer, *Cell* **43**, 143 (1985).
19. J. R. Nevins, *Annu. Rev. Biochem.* **52**, 441 (1983); A. L. Beyer and Y. N. Osheim, *Semin. Cell Biol.* **2**, 131 (1991). There is evidence for and against the cotranscriptional splicing of precursor mRNAs. Beyer has shown that nascent transcripts in *Drosophila* are associated with spliceosomes, and in some cases, the spliceosome and nascent transcripts can be directly visualized by electron microscopy. In contrast, Nevins and others have shown that the unspliced transcripts in mammalian cells can be isolated in the poly(A) fraction, which indicates that splicing is posttranscriptional.
20. C. V. Johnson, J. A. McNeil, K. C. Carter, J. B. Lawrence, *Genet. Anal. Tech. Appl.* **8**, 75 (1991). The two-color filter was made by Chroma Technology, Brattleboro, VT; C. V. Johnson, R. Singer, J. R. Lawrence, *Methods Cell Biol.* **35**, 73 (1992).
21. D. C. Tkachuk *et al.*, *Science* **250**, 559 (1990).
22. Because of their abundant cytoplasm, fibroblasts and myoblasts were extracted with Triton X-100, a treatment that may preferentially release excised intron sequences from the nucleus (*23*). The presence of fibronectin mRNA in the fibroblast perinuclear cytoplasm made it difficult to evaluate whether there was a low concentration of exons throughout the nucleoplasm. The PC-12 cells were easier to evaluate because they have little cytoplasm and did not need to be detergent-extracted.
23. S. Zeitlin, A. Parent, S. Silverstein, A. Efstratiadis, *Mol. Cell. Biol.* **7**, 111 (1987); C. Coleclough and D. Wood, *ibid.* **4**, 2017 (1984).
24. The nuclear volume occupied by all of the poly(A) domains in a given nucleus is estimated to be 5% (*6*), whereas the specific RNA accumulations occupy no more than 1%. Hence, the frequency with which fibronectin RNA would spatially associate with these domains by random chance is small. The specificity of association is further demonstrated by previous experiments showing that nontranscribed centromeric sequences are not associated with poly(A) domains (*7*).
25. Because poly(A) RNA is detected with a small (55 bp) oligonucleotide end-labeled with only a few biotin molecules and the fibronectin RNA is detected by much larger (1 to 6 kb) probes labeled throughout by nick-translation, the amount of fluorescence generated per molecule with the poly(A) probe is much less (at least an order of magnitude) than that generated with the fibronectin mRNA probe. Nevertheless, rough measurements of the relative intensity and size of individual poly(A) RNA domains indicate that the domains contain substantially more fluorescent signal (and hence many more RNA molecules) than individual RNA foci or tracks do. This consideration, along with the observation that fibronectin RNA tracks only partially overlap the transcript domains, supports the conclusion that each transcript domain is likely to be the transcription and processing site of several RNAs.
26. J. R. Coleman and J. B. Lawrence, unpublished data; Y. Xing and J. B. Lawrence, unpublished data. Several but not all active sequences studied are associated with domains.
27. We thank R. Hynes, J. Schwarzbauer, D. Shapiro, and P. Norton for providing SX19-3 and C1A1, BBG-5′BR, pFH-1, and G1-4.9 clones, respectively; T. Maniatis for supplying antibody to SC-35; C. Beaudry for help with manuscript preparation; C. Dunshee for excellent and patient assistance in photographic processing; and J. McNeil for expertise in computer imaging. Supported by Research Career Development Award grant from NIH National Center for Human Genome Research (J.B.L.), by NIH grant RO1 HG00251 (J.B.L.), and by NIH grant RO1 HL33307 (P.R.D.).

14 July 1992; accepted 22 December 1992

A Three-Dimensional View of Precursor Messenger RNA Metabolism Within the Mammalian Nucleus

Kenneth C. Carter, Douglas Bowman, Walter Carrington, Kevin Fogarty, John A. McNeil, Fredric S. Fay, Jeanne Bentley Lawrence*

A quantitative three-dimensional analysis of nuclear components involved in precursor messenger RNA metabolism was performed with a combination of fluorescence hybridization, immunofluorescence, and digital imaging microscopy. Polyadenylate [poly(A)] RNA-rich transcript domains were discrete, internal nuclear regions that formed a ventrally positioned horizontal array in monolayer cells. A dimmer, sometimes strand-like, poly(A) RNA signal was dispersed throughout the nucleoplasm. Spliceosome assembly factor SC-35 localized within the center of individual domains. These data support a nuclear model in which there is a specific topological arrangement of noncontiguous centers involved in precursor messenger RNA metabolism, from which RNA transport toward the nuclear envelope radiates.

Nuclei of higher eukaryotic cells must transcribe, process, and selectively transport several major classes of RNA including mRNA, ribosomal RNA (rRNA), tRNA, and small nuclear RNA. The transcription and processing of rRNA are confined to the nucleolus (*1*), but the subnuclear location of metabolism for other RNA classes including precursor mRNA (pre-mRNA) remains unresolved (*2–10*). Recent evidence